Sensors & Transducers, Vol. 154, Issue 7, July 2013, pp. 195-200

www.sensorsportal.com

Sensors & Transducers

http://www.sensorsportal.com

Morphology Control of Tin Oxide Nanostructures and Sensing Performances for Acetylene Detection

[1*] Weigen CHEN, [1*] Qu ZHOU, [2] Xiaoping SU, [1] Lingna XU, [3] Shudi PENG

[1] State Key Laboratory of Power Transmission Equipment & System Security and New Technology, Chongqing University, Chongqing, 400030, China

[2] Chengdu Power Supply Company, Sichuan, 610017, China

[3] Chongqing Electric Power Research Institute, Chongqing, 401123, China

[1] Tel.: +86-23-65111172, fax: +86-23-65111172

E-mail: weigench@cqu.edu.cn, zhouqu@cqu.edu.cn, xiaopingsu@cqu.edu.cn, lingnaxu@cqu.edu.cn, psdzq@yahoo.cn

Received: 21 May 2013 /Accepted: 19 July 2013 /Published: 31 July 2013

Abstract: Morphology Control plays an important role in gas sensing properties of metal oxide semiconductor based gas sensors. In this study, various morphologies of SnO_2 nanostructures including nanobulks, nanospheres, nanorods, and nanowires were successfully synthesized via a simple hydrothermal method assisted with different surfactants. X-ray powder diffraction and scanning electron microscopy were employed to characterize the prepared products. Gas sensors were fabricated by screen-printing the as-prepared SnO_2 nanostructures onto planar ceramic substrates. Moreover, their gas sensing properties were systematically investigated towards acetylene gas (C_2H_2), an important fault hydrocarbon dissolved in power transformer oil. Experiments indicate that the SnO_2 nanowires based sensor exhibits excellent gas sensing properties, such as lower operating temperature, higher gas response, quicker response-recovery time and good stability than those of SnO_2 nanobulks, nanospheres and nanorods. These results imply SnO_2 nanowires a promising sensing morphology for C_2H_2 detection and provide us a feasible way to develop high-performance gas sensor by tailoring the microstructures and morphologies of the materials in further. *Copyright © 2013 IFSA.*

Keywords: SnO_2 nanostructures, Gas sensor, Acetylene, Gas sensing properties.

1. Introduction

Large-scale power transformers are expensive and significant electric apparatus in power transmission and distribution system [1, 2]. As one of the most important fault characteristic gases dissolved in transformer oil, acetylene (C_2H_2) can effectively reflect the incipient faults of partial discharge [3, 4]. Therefore, how to rapidly and accurately detect dissolved C_2H_2 in oil is currently the subject of intensive research [5].

In recent years, great efforts have been made to this field and numerous methods, including metal oxide semiconductor (MOS) [6], infrared spectroscopy [7], Raman spectroscopy [8] or photoacoustic spectroscopy [9] and carbon nanotube [10] have been employed for C_2H_2 detection. Owning to the remarkable advantages of simple design technology, easy fabrication process, low maintenance cost and long service life, MOS has proved to be a promising gas sensing material [11]. However, some limitations still need to be further

improved, such as high operating temperature, low gas response and poor long-term stability.

Recently, interest in morphology control of MOS has been greatly stimulated. And different morphologies of MOS including wires [12], flowers [13], rods [14], spheres [15], fibers [16] and tubers [17] have been prepared. However, to the best of our knowledge, reports on the synthesis of various SnO_2 nanostructures by hydrothermal method assisted with different surfactants have been rare and there are no literatures on morphology control of various SnO_2 nanostructures and its application as a C_2H_2 gas sensor.

In this study, we first reported a simple and facile hydrothermal method assisted with different surfactants to prepare variety morphologies of SnO_2 nanostructures. Then X-ray powder diffraction (XRD) and scanning electron microscopy (SEM) were employed to characterize the prepared samples and a possible growth mechanism was discussed in detailed. Finally, gas sensors were fabricated with a planar structure and C_2H_2 sensing properties were systematically measured.

2. Experimental

2.1. Synthesis of SnO_2 Nanostructures

All the raw chemicals were analytical-grade reagents purchased from Chongqing Chuandong Chemical Reagent Co. Ltd. and used as received without any further purification. Various morphologies of SnO_2 nanostructures including nanobulks, nanospheres, nanorods, and nanowires were successfully synthesized with a facile surfactant-assisted hydrothermal method. The detailed synthesis processes were as follows:

In a typical synthesis process of SnO_2 nanospheres: 1.4 g of $SnCl_4 \cdot 5H_2O$, 1.24 g of NaOH and 0.16 g of citric acid were dissolved completely into 60 mL mixture of absolute ethanol and distilled water (1/1, V/V) in a 100 mL capacity beaker under intense magnetic stirring. Then the mixed solution was transferred into a 100 mL Teflon-lined stainless steel autoclave, sealed and maintained at 180 °C for 24 h in an electric furnace. When the reaction was completed, the autoclave was cooled to room temperature naturally. The product was harvested by centrifugation, washed with distilled water and absolute ethanol several times, respectively, and dried at 60 °C in air to remove the solvent.

SnO_2 nanorods and nanowires were obtained in a similar process except that 0.2 g of polyvinyl pyrrokidone (PVP, K30 g) and 0.1 g of polyethylene glycol (PEG, MW = 6,000) were added to replace citric acid, respectively. SnO_2 nanobulks were prepared by the following process: 1.4 g of $SnCl_4 \cdot 5H_2O$, 0.6 g of $CO(NH_2)_2$, 0.15 g of glycine, 30 mL absolute ethanol and 30 mL distilled water were mixed together under intense magnetic stirring, and then the precipitation precursor was transferred into a 100 mL Teflon-lined stainless steel autoclave, sealed and maintained at 160 °C for 20 h. The product was obtained by cooling, centrifugation, washing and drying.

2.2. Structure Characterization

The crystalline structures of the prepared products were investigated with X-ray powder diffraction (XRD) using a Rigaku D/Max-1200X diffractometer (Tokyo, Japan) with Cu Kα radiation (40 kV, 200 mA and λ = 1.5418 Å) and 2θ ranging from 20° to 80°. The surface morphologies of the nanostructures were characterized with a Nova 400 Nano field emission scanning electron microscope (FE-SEM, FEI, Hillsboro, OR, USA). A surface area and porosimetry analyzer (V-Sorb 2800, Beijing Jinaipu General Instrument Co., Ltd, Beijing, China) was employed to test the specific surface area and open pore size of the nanostructures.

2.3. Fabrication of Gas Sensor

The synthesized SnO_2 nanostructures were firstly ground into fine powder and mixed with absolute ethanol and deionized water in a weight ratio of 8:1:1 to form a paste. Then the paste was screen-printed onto a planar ceramic substrate, where five pairs of Ag-Pd interdigital electrodes had been pre-deposited. Finally, the sensor was dried in air at 60 °C to volatilize the organic solvent and further aged in an aging chamber for 36 h. Fig. 1 shows the structural scheme of the planar sensor.

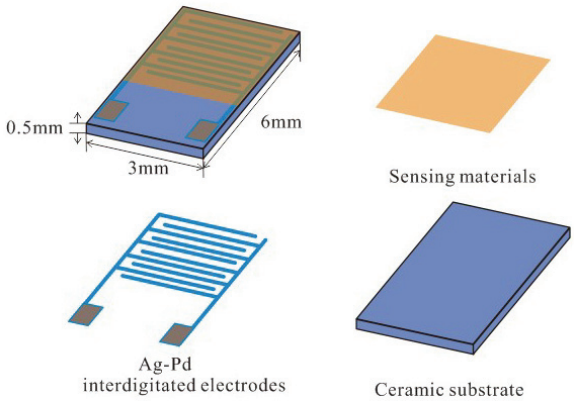

Fig. 1. Structure representation of the planar gas sensor.

2.4. Gas Sensing Property Measurement

Gas sensing properties of the prepared SnO_2 based sensors towards C_2H_2 were measured by a CGS-1TP intelligent gas sensing analysis system purchased from Beijing Elite Tech Co., Ltd, China which could offer an external temperature control

ranging from room temperature to 500 °C with an adjustment precision of 1 °C. Fig. 2 shows a top-view photograph of the operating platform.

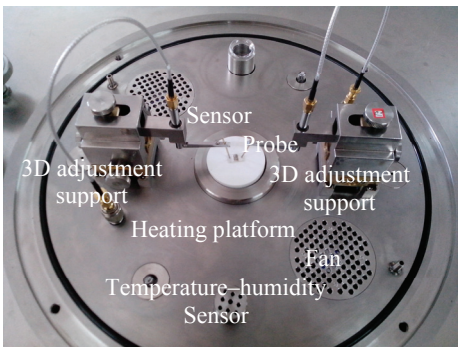

Fig. 2. A top-view photograph of the operating platform in CGS-1TP.

As seen in Fig. 2 the planar sensors were laid on the heating platform and two adjustable probes were pressed on the sensor electrodes to collect electrical signals. When the sensor was pre-heated at certain operating temperature for about 30 min and its resistance was stable, saturated target gas was injected into the test chamber (18 L in volume) by a micro-injector through a rubber plug. The saturated target gas was mixed with air in the test chamber by two fans. After its resistance value reached a new constant value, the test chamber was opened to recover the sensor in air.

The gas response S was defined as $S = R_a/R_g$, where R_a was the electrical resistance value of prepared planar sensor in air and R_g was that in a mixture of target gas and air. The time taken by the sensor to reach 90 % of the total resistance change was defined as the response time in the case of gas adsorption or the recovery time in the case of gas desorption. All measurements were repeated several times to ensure the repeatability and stability of the sensor.

3. Results and Discussion

3.1. Structural Characterization

X-ray powder diffraction (XRD) measurement was first employed to characterize the crystalline structure and chemical composition of the prepared nanotructures. As shown in Fig. 3 the prominent peaks (110), (101), (211) and other smaller peaks are highly consistent with the standard data file of rutile SnO_2 (JCPDS file no. 41-1445). No diffraction peaks from any impurities were observed, implying a high purity of our prepared samples.

Field emission scanning electron microscopy (FESEM) was further used to investigate the morphologies and microstructures of the synthesized samples. Fig. 4 (a) shows a typical SEM image of spherical SnO_2 nanostructures, which are uniform in size and shape and the average diameters range from 300 nm to 400 nm. Fig. 4 (b) shows the SEM image of SnO_2 nanobulks with average thickness of 150 nm. Fig. 4 (c) displays a SEM image of the synthesized SnO_2 nanorods. It can be clearly seen in Fig. 4 (c) that flower-like sample is composed of a large scale of nanorods with width of about 150 nm and length of 500-600 nm. The SEM image of SnO_2 nanowires is shown in Fig. 4 (d), where the lengths of the nanowires range from hundreds of nanometers to several ten micrometers and the mean diameters are in the scope of 80 to 120 nm. These results indicate that different morphologies of SnO_2 nanostructures have been successfully obtained under the current synthetic conditions.

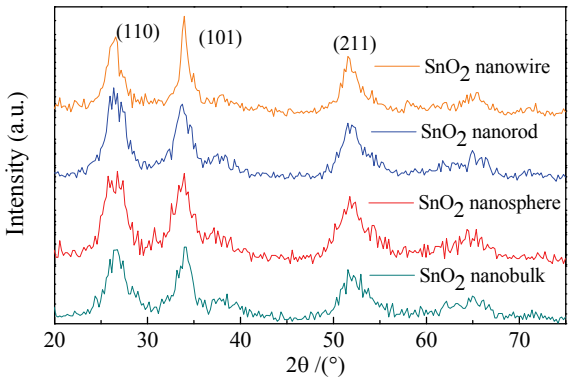

Fig. 3. XRD patterns of the prepared SnO_2 nanostructures.

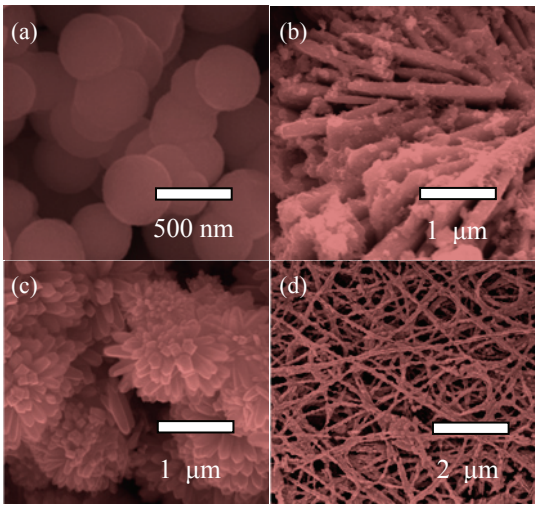

Fig. 4. FESEM images of the prepared SnO_2 nanostructures (nanobulks (a), nanospheres (b), nanorods (c), and nanowires (d)).

3.2. Growth Mechanism

According to the experiments of material synthesis and structural characterization, surfactant added in the precursor plays an important role in the

final morphologies of the as-prepared products. In order to reveal how the additive surfactants affect the morphologies of the prepared SnO_2 nanostructures, possible growth mechanisms are discussed in the following section.

The whole growth process can be divided into a nucleation stage and a self-assembly stage. The former is closely related to the reaction solvents, while the latter is mainly depends on the surface-active agents. A certain amount of $Sn[(OH)_6]^{2-}$ ions has been reported recently as a prerequisite for hydrothermal synthesis of rutile SnO_2 nanostructures. The chemical reactions for the formation of the SnO_2 precursor in our programs can be described as:

$$Sn^{4+}+6OH^{-}\rightarrow Sn[(OH)_6]^{2-}\rightarrow SnO_2+2H_2O+2OH^{-}$$

At first a large number of tiny SnO_2 nanoparticles was formed spontaneously from the dehydration of abundant component $Sn[(OH)_6]^{2-}$ ions. With the reaction time increasing, the tiny SnO_2 crystal nanoparticles gathered and develop into larger nanocrystals. Thus, SnO_2 nanospheres were observed in Fig. 4 (a) with no addition of any surfactant. With the addition of glycine, SnO_2 nanobulks were obtained as seen in Fig. 4 (b). It could be considered that glycine benefited the growth along one direction and agglomerated the nanoparticles to form smooth bulks.

When PVP was added to the reaction solvent SnO_2 nanorods were firstly produced with the assistance of polarized functional groups (–C=O) [18], which were commonly present in PVP. These prepared nanorods subsequently aggregated with the common centre of PVP. Finally, flower-like SnO_2 nanostructures appeared [19]. As known to all PEG is a kind of template with long chains, and numerous of hydrophilic "–O–" and "$–CH_2–CH_2–$" groups exist along its long chains [20]. With the addition of PEG, numerous of tiny $Sn[(OH)_6]^{2-}$ crystals embed and nucleated in the long-chains of PEG. Thus, net-like SnO_2 nanowires were successfully synthesized.

3.2. Gas Sensing Properties

In order to make clear how the morphologies of SnO_2 nanostructures influence the gas sensing behaviors of the SnO_2 based sensors, systematic C_2H_2 sensing experiments, including operating temperature, gas response, response-recovery time, stability and repeatability were measured.

The gas responses of the prepared SnO_2 based sensors to 100 μL/L of C_2H_2 as a function of operating temperature ranging from 100 to 430 °C are measured in Fig. 5 to find out the optimum operating temperature. As shown in Fig. 5 for each sensor curve, the gas response increases first at different degrees and reaches its maximum value, and then decreases rapidly with further increasing temperature. The optimum operating temperatures of nanobulks and nanospheres based sensors are tested to be about 280 °C, while 250 °C for nanorods and nanowires, where the sensor exhibits the maximum gas responses of 20.34, 26.80, 34.04 and 46.96 respectively.

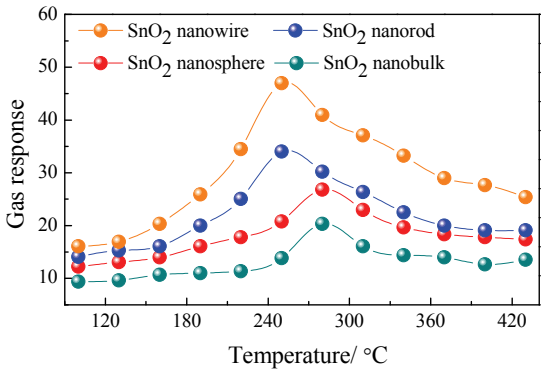

Fig. 5. Response versus operating temperature of the sensors to 100 μL/L of C_2H_2.

Fig. 6 shows the gas responses of the nanowire and nanobulk SnO_2 based sensors towards C_2H_2 with gas concentration ranging from 1μL/L to 1000 μL/L. As can be seen, the gas response of the SnO_2 nanowires (operated at 250 °C) increases rapidly in linearity with increasing C_2H_2 concentration below 200 μL/L. And then the sensor shows a slower increase with further increasing the gas concentration, and finally reaches saturation at nearly about 1000 μL/L. Similar C_2H_2 response curves were also found for SnO_2 nanobulk based sensor (operated at 280 °C), while much weaker.

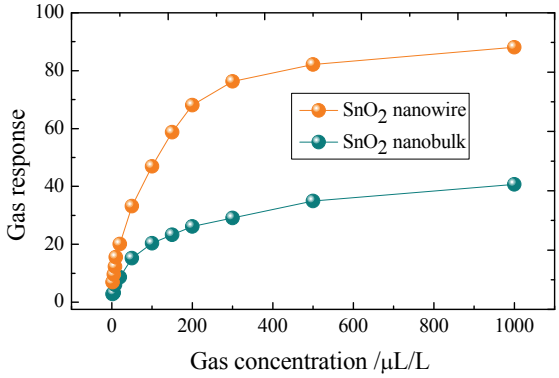

Fig. 6. Responses of SnO_2 nanowire and nanobulk sensor versus C_2H_2 concentration from 1 to 1000 μL/L.

Responds and recovery time is another key gas sensing parameter of metal oxide semiconductor gas sensor. Fig. 7 shows the transient responses of various SnO_2 based sensors exposed to 20 μL/L of C_2H_2 with sensor working at its optimum operating temperature. The response-recovery time of nanobulks, nanospheres, nanorods, and nanowires based sensors were calculated to be about 15-25, 13-21, 11-18, 7-13 s, respectively.

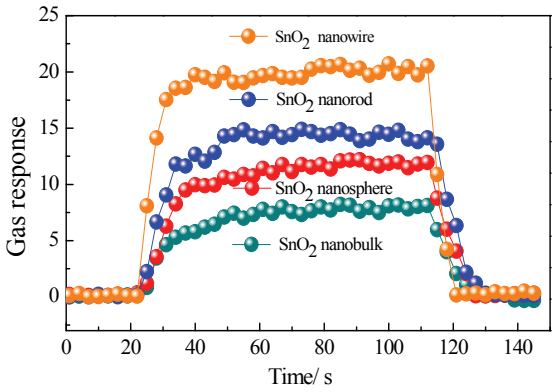

Fig. 7. Response and recovery characteristics of the sensor to 20 μL/L of C_2H_2.

The long-time stability and repeatability of the sensors have been also measured as shown in Fig. 8. One can clearly see that the prepared SnO_2 nanowires sensor changes slightly and exhibits a nearly constant sensing response during the long experimental cycles, confirming the excellent stability and good repeatability of the SnO_2 nanowires sensor for C_2H_2 detection.

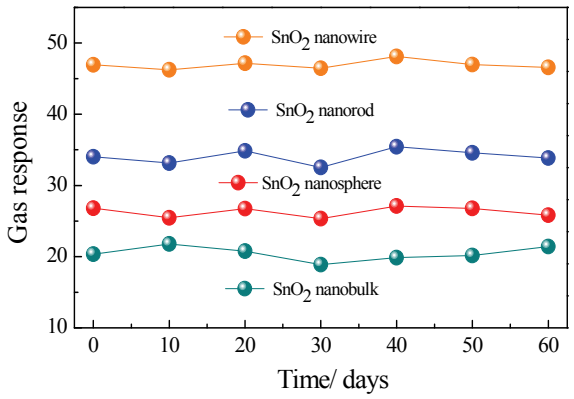

Fig. 8. Long-time stability of the prepared sensors to 100 μL/L of C_2H_2.

It is known to all that rutile SnO_2 is an important n-type semiconductor sensing material and the change in electrical resistance is dominantly controlled by the adsorption and desorption process of C_2H_2 molecules on SnO_2 surface. Due to the nonstoichiometry of the prepared SnO_2 nanostructures, many oxygen vacancies exist in their crystal lattices. When the SnO_2 based sensors were surrounded by air, oxygen molecules would be absorbed on the sensing surface to generate various kinds of chemical adsorbed oxygen species, including O_2^-, O^{2-} and O^-. Thus the sensor would exhibit a high electrical resistance. When the sensor was exposed certain concentration of C_2H_2 atmosphere, a typical reducing gas, a reaction happened between the adsorbed oxygen and C_2H_2 molecule. Meanwhile, the adsorbed electrons are released to SnO_2 surface, which decreases the height of barrier in the depletion region and increases the carrier concentration. Therefore, a decreasing electrical resistance of the sensor was measured. A possible gas sensing process between the prepared SnO_2 nanostructures and C_2H_2 gas in this study can be expressed as follows [21].

$$O_{2gas} \rightarrow O_{2ads}$$
$$O_{2ads} + e^- \rightarrow O_{2ads}^- \ (T<100°C)$$
$$O_{2ads}^- + e^- \rightarrow 2O_{ads}^- \ (100<T<300°C)$$
$$O_{ads}^- + e^- \rightarrow O_{ads}^{2-} \ (300°C<T)$$
$$C_2H_2(gas) \rightarrow C_2H_2(ads)$$
$$C_2H_2(ads) + 5O_{ads}^- \rightarrow CO_2(gas) + H_2O(gas) + 5e^-$$

To go insight into how the nanostructures and morphologies of the as-prepared SnO_2 samples influence C_2H_2 sensing behaviors, nitrogen adsorption and desorption measurements were further employed to estimate the texture properties. With the Barrett–Joyner–Halenda method [22], the BET surface area and pore structure parameters are calculated and shown in Table 1. With larger BET surface area and pores compared with those of nanobulks, nanospheres and nanorods, SnO_2 nanowires would provide much more reaction sites and promote charge transfer in the sensing process. Thus, excellent C2H2 sensing properties are observed in our measurements.

Table 1. BET surface area and pore structure parameters of the samples.

SnO_2	S_{BET} (m^2g^{-1})	d_P (nm)
Nanowire	27.4	9.2
Nanorod	21.9	8.7
Nanobulk	17.6	6.8
Nanosphere	14.3	5.4

4. Conclusions

Various morphologies of SnO_2 nanostructures, including nanobulks, nanospheres, nanorods, and nanowires have been successfully prepared and performed with XRD and FESEM. Planar SnO_2 based gas sensors were fabricated with screen-printing and their gas sensing properties were systematically measured towards C_2H_2. The optimum operating temperatures of nanobulks, nanospheres, nanorods and nanowires are suggested to be about 280, 280, 250 and 250 °C. The corresponding response value of the sensors towards 100 μL/L of C_2H_2 are tested to be about 20.34, 26.80, 34.04 and 46.96 respectively and the response-recovery time are calculated to be about 15-25, 13-21, 11-18, 7-13 s, respectively. The prepared nanowires exhibit excellent gas sensing properties that those of nanobulks, nanospheres and nanorods, which implies a promising sensing morphology in fabricating high-performance C_2H_2 gas sensor.

Acknowledgements

This work was supported in part by the National Natural Science Foundation of China (No. 51277185, No. 51202302), the Funds for Innovative Research Groups of China (No. 51021005) and China Postdoctoral Science Foundation (No.2012M511904).

References

[1]. R. Rogers, IEEE and IEC codes to interpret incipient faults in transformers, using gas in oil analysis, *IEEE Transactions on Electrical Insulation,* Vol. 13, Issue 5, 1978, pp. 349-354.

[2]. W. G. Chen, Study on the technology of on-line monitoring and fault diagnosis for transformer insulation using the character value of oil-dissolved gases, *Chongqing University*, Chongqing, China, 2003.

[3]. S. Singh, M. Bandyopadhyay, Dissolved gas analysis technique for incipient fault diagnosis in power transformers: a bibliographic survey, *IEEE Electrical Insulation Magazine,* Vol. 26, Issue 6, 2010, pp. 41-46.

[4]. M. Wang, A. J. Vandermaar, K. D. Srivastava, Review of condition assessment of power transformers in service, *IEEE Electrical Insulation Magazine,* Vol. 18, Issue 6, 2002, pp. 12-25.

[5]. S. Fei, M. J. Wang, Y. Miao, C. Liu, Particle swarm optimization-based support vector machine for forecasting dissolved gases content in power transformer oil, *Energy Conversion and Management,* Vol. 50, Issue 6, 2009, pp. 1604-1609.

[6]. N. Tamaekong, C. Liewhiran, A. Wisitsoraat, S. Phanichphant, Acetylene sensor based on Pt/ZnO thick films as prepared by flame spray pyrolysis, *Sensors and Actuators B: Chemical,* Vol. 152, Issue 2, 2011, pp. 155-161.

[7]. W. G. Chen, Y. X. Yun, C. Pan, Analysis of infrared absorption properties of dissolved gases in transformer oil, in *Proceedings of the CSEE,* Vol. 28, Issue 16, 2008, pp. 148-153.

[8]. X. Y. Li, Y. X. Xia, J. M. Huang, L. Zhan, A Raman system for multi-gas-species analysis in power transformer, *Applied Physics B,* Vol. 93, Issue 3, 2008, pp. 665-669.

[9]. Y. X. Yun, W. G. Chen, Y. Y. Wang, C. Pan, Photoacoustic detection of dissolved gases in transformer oil, *European Transactions on Electrical Power,* Vol. 18, Issue 6, 2008, pp. 562-576.

[10]. X. X. Zhang, J. B. Zhang, J. Tang, F. S. Meng, W. T. Liu, Ni-doped carbon nanotube sensor for detecting dissolved gases in transformer oil, in *Proceedings of the CSEE,* Vol. 31, Issue 4, 2011, pp. 119-124.

[11]. Q. Zhou, W. G. Chen, L. N. Xu, S. D. Peng, Study on Sensing Properties and Mechanism of Pd-doped SnO_2 Sensor for Hydrogen and Carbon Monoxide, *Sensors & Transducer,* Vol. 151, Issue 4, April 2013, pp. 84-89.

[12]. V. Kumar, S. Sen, KP. Muthe, N. Gau, S. Gupta, J. Yakhmi, Copper doped SnO2 nanowires as highly sensitive H_2S gas sensor, *Sensors and Actuators B: Chemical,* Vol. 138, Issue 2, 2009, pp. 587-590.

[13]. J. R. Huang, K. Yu, C. P. Gu, M. H. Zhai, Y. J. Wu, M. Yang, J. H. Liu, Preparation of porous flower-shaped SnO_2 nanostructures and their gas-sensing property, *Sensors and Actuators B: Chemical*, Vol. 147, Issue 2, 2010, pp. 467-474.

[14]. S. Shinde, G. Patil, D. Kajale, V. Gaikwad, Synthesis of ZnO nanorods by spray pyrolysis for H_2S gas sensor, *Journal of Alloys and Compounds,* Vol. 528, Issue 5, 2012, pp. 109-114.

[15]. Z. P. Li, Q. Q. Zhao, W. L. Fan, J. H. Zhan, Porous SnO2 nanospheres as sensitive gas sensors for volatile organic compounds detection, *Nanoscale*, Vol. 3, Issue 4, 2011, pp. 1646-1652.

[16]. J. Gong, Y. H. Li, Z. S. Hu, Z. Z. Zhou, Y. L. Deng, Ultrasensitive NH3 gas sensor from polyaniline nanograin enchased TiO2 fibers, *The Journal of Physical Chemistry C,* Vol. 114, Issue 21, 2010, pp. 9970-9974.

[17]. X. X. Zhang, J. B. Zhang, R. H. Li, Y. F. Liao, Application of hydroxylated single-walled carbon nanotubes for the detection of C_2H_2 Gases in Transformer Oil, *Journal of Computational and Theoretical Nanoscience,* Vol. 10, Issue 2, 2013, pp. 399-404.

[18]. C. Xia, N. Wang, L. Wang, L. Guo, Synthesis of nanochain-assembled ZnO flowers and their application to dopamine sensing, *Sensors and Actuators B: Chemical,* Vol. 147, Issue 2, 2010, pp. 629-634.

[19]. M. Zeng, H. H. Yin, K. Yu, Synthesis of V_2O_5 nanostructures with various morphologies and their electrochemical and field-emission properties, *Chemical Engineering Journal,* Vol. 188, Issue 15, 2012, pp. 64-70.

[20]. Y. X. Yin, L. J. Jiang, L. J. Wan, C. J. Li, Y. G. Guo, Polyethylene glycol-directed SnO_2 nanowires for enhanced gas-sensing properties, *Nanoscale*, Vol. 3, Issue 4, 2011, pp. 1802-1806.

[21]. T. P. Chen, S. P. Chang, F. Y. Hung, S. J. Chang, Z. S. Hu, K. J. Chen, Simple fabrication process for 2D ZnO nanowalls and their potential application as a methane sensor, *Sensors*, Vol. 13, Issue 3, 2013, pp. 3941-3950.

[22]. Z. H. Jing, J. H. Zhan, Fabrication and gas-sensing properties of porous ZnO nanoplates, *Advanced Materials,* Vol. 20, Issue 23, 2008, pp. 4547-4551.